Review Article
cnj.araku.ac.ir

☑ Cite This: Colloid Nanosci. J. 3(2) (2025) 622-638 DOI: 10.61882/CNJ.3.2.622

Effect of Initial Temperature on the Efficiency of Asphaltene Adsorption Onto Lime Nanoparticles: A Molecular Dynamics Study

Hossein Namdari[1], Mojtaba Rahimi[1,2]*

[1] Department of Petroleum Engineering, Kho.C., Islamic Azad University, Khomeinishahr, Iran
[2] Stone Research Center, Kho.C., Islamic Azad University, Khomeinishahr, Iran

ARTICLE INFO

Article History:
Received 2025-09-16
Revised 2025-12-01
Accepted 2025-12-09
Published 2025-09-01

Corresponding Authors:
Mojtaba Rahimi
Email:
mrahimi@iau.ac.ir

ABSTRACT

For its main purpose, this work used molecular dynamics simulations to study the adsorption behavior of asphaltene molecules on lime nanoparticles in a water medium at different initial temperatures. The major objective of this research was to find out the role of temperature on the efficiency, strength, and mechanism of asphaltene adsorption onto lime nanoparticles, which are naturally good candidates for the mitigation of asphaltene precipitation in upstream and midstream systems of the petroleum industry. Atomic models incorporated asphaltene molecules and 20 wt% lime nanoparticles and allowed to equilibrate for 10 ns to bring the system close to thermodynamic stability with an average temperature of 299.44 K and kinetic energy of 0.86 kcal/mol. Further adsorption simulations for an additional 10 ns produced very good results, where asphaltenes were found to saturate, reaching a maximum atomic density of 180.72 atoms/Å^3 close to the surfaces of the nanoparticles, and an interaction energy of 0.047 kcal/mol, showing that they had formed a very stable adsorption configuration. As much as 69% of the asphaltene molecules would have already stuck to nanoparticle surfaces during the first 7 ns before they approached saturation. The maximum atomic density reduced from 300 K to 350 K to reach a value of 161.37 atoms/Å^3, the interaction energy decreased to 0.031 kcal/mol, and the adsorption ratio decreased from 69% to 56%, evidence of a temperature-dependent reduction in adsorption efficiency. These findings will shed light on the molecular-level thermal sensitivity aspects of asphaltene strategies based on lime-nanoparticle control. In addition, they will support the development of more efficient nanofluid formulations for petroleum-related applications.

KEYWORDS: *Lime Nanoparticle, Asphaltene Adsorption, Temperature, Molecular Dynamics Simulations*

1. Introduction

Asphaltene deposition is one of the chief problems in the oil industry. It is always persistent and multifaceted, keeping up with considerable damage to reservoir performance, permeability reduction, well and pipeline plugging, and processing equipment damage [1, 2]. It is the densest fraction of crude oil featuring highly complex polyaromatic and polar molecular structures that may contain heteroatoms like nitrogen, sulfur, oxygen, and trace metals such as nickel and vanadium, in addition to hydrocarbons [3, 4]. It is thermodynamically stable in a changing T, pressure, and fluid composition environment, which allows aggregation, flocculation, and precipitation [5]. Recently, NPs were recommended as adsorbents for controlling and reducing asphaltene deposition in petroleum systems [6, 7]. The high proportion of surface area versus the volume, changeable surface chemistries, nanoscale dimensions, and inherent compatibility with porous media allow them to be the best use in relation to those highly complex and polar

asphaltene molecules [7, 8]. In petroleum systems, NPs used for asphaltenes adsorption were most commonly classified into two main categories: synthetic and naturally occurring mineral NPs. Synthetic NPs, generally metalliferous or metal-oxide-based, were known for their thermal and chemical stability, ability to preserve crystalline architecture, and customizable surface chemistry. These properties allowed them to form strong bonds with asphaltenes' polar and aromatic constituents through hydrogen bonding, electrostatic interaction, and π-π interaction, respectively, thus increasing their adsorption efficiency [9, 10]. The naturally occurring mineral NPs, on the other hand, had some other advantages derived from their geological ubiquity, such as intrinsic porosity, mechanical strength, environmental compatibility, and economic viability. Although their surface chemistry was less amenable to modification than their synthetic equivalents, such natural NPs can likewise be developed in ways to enhance their interaction with asphaltenes [11, 12]. Hence, it is vital to have an excellent understanding of the structural and chemical properties of NPs when selecting and developing the most efficient adsorbents for minimizing asphaltene deposition, particularly under variable and complex reservoir conditions [13].

MD simulations were used by Zhu et al. [14] to probe the effects of different water contents on the states of asphaltene aggregation and the rheological properties of crudes. Their investigation confirmed that increasing the concentration of water caused a transition from bulk-phase asphaltene assemblages to interfacial adsorption that produced water-in-oil emulsions. Lu et al. [15] investigated the silica aerogel NPs for oil recovery improvement and asphaltene deposition mitigation in carbon capture, utilization, and storage (CCUS) processes. Sandpack tests revealed that the addition of such NPs resulted in increased oil recovery from 49.39% to 73.21% and CO_2 sequestration efficiency from 45.35% to 83.37%. The NPs migrated into the oil phase and altered the interfacial properties to stabilize CO_2-in-oil foams with associated reductions in CO_2 mobility. Molecular simulations showed that aerogel pores could adsorb asphaltene molecules and prevent their deposition. Shadervan et al. [16] investigated surface-modified silica and $CaCO_3$ NPs as asphaltene precipitation inhibitors and oil-recovery enhancers. Their results reveal that both NPs delay asphaltene precipitation onset; however, calcium carbonate performed much better at low amounts by suspending asphaltenes, while silica was more successful at high concentrations. Wettability and interfacial tension test results established the optimal working concentration for each NP. Silica NPs had much higher colloidal stability and could attain up to a maximum oil recovery rate of 33% at 0.1 wt.%. In contrast, calcium carbonate was limited to maximum oil recovery of 25% at 0.01 wt.%. Torki et al. [17] had used MD simulations in investigating the effect of using Fe_3O_4-NPs on asphaltene adsorptions in heavy oils, an approach intended to solve the problem of asphaltene precipitation causing formation damage to areas near wellbores. Their results indicated that the gradual increase in the NPs concentration from 2.5% to 7% improved diffusion, displacing, atomic density, and adsorption rate, and thus increased asphaltene inhibition from 72% to 79%. Hayatizadeh et al. [18] relied on MD simulations, where asphaltene NPs were aggregated in the full hydrophilic SiO_2-NP presence at 1 and 300 bar pressures. Asphaltene molecules were found to strongly adsorb at the NPs surfaces by their aromatic rings and polar groups and result in a reduction up to 85% in asphaltene-asphaltene interactions and very efficiently inhibit aggregation. What was more, the NPs tended to cluster under aromatic solvents, as toluene was, in contrast to their-iliphatic solvents like heptane, demonstrating the influence of oil composition on NP behavior.

The effects of asphaltene adsorption on understanding the proper use of chosen NPs are prerequisites for developing efficient control strategies for the petroleum systems design. Recent advances in computational techniques, especially MD simulations, have allowed in-depth investigations on the scale of intermolecular interactions at the nanoscale [19, 20]. The present study was intended to have an empirical evaluation of initial T effects on the fate and mechanism of asphaltene adsorption onto lime NPs using MD simulation techniques. An innovative approach was developed here to analyze the process of adsorption of asphaltenes on lime NP surfaces based on property changes under varying Ts, such as atomic density distribution, IE, and adsorption kinetics. This enabled the understanding of the effect of T on the interaction mechanisms in the asphaltene molecule and lime NPs and was important for developing effective handling strategies to control

and mitigate asphaltene deposition. This article used MD simulations to analyze the performance of asphaltene molecules adsorbing onto lime NPs at different initial Ts and conditions. The main focus was to unveil the mechanisms involved in adsorption and how asphaltenes interact with lime NPs. Results from this study would shed light on the impact of functionalization of NP-based strategies for industrial use, leading to enhanced performance and quality in asphaltic and petroleum systems.

2. MD simulation

MD simulation is a powerful method to study the time-dependent behavior of atoms and molecules in complex systems. It applies the laws of classical mechanics to describe how particles move and interact with other particles under the influence of different forces. The simulation typically begins by placing the particles at specific positions and giving them specific velocities, which would change as the system evolves due to internal and external interactions. These interactions have several different types of physical origin, from electrostatic attractions or repulsions among charged species to non-bonded interactions, such as dispersion forces. By determining the way these forces operate on the motion of each particle over time, MD simulation creates the avenue for an atomistic view of certain dynamic processes at the nanoscale [21].

$$F_i = m_i a_i = -\nabla_i U = -\frac{dU}{dr_i} \quad (1)$$

Understanding the intricate motions of atoms inside molecular systems requires working with advanced computational techniques, mainly because of factors such as T fluctuations, pressure changes, and intermolecular forces. Conventional analytical techniques often fail to capture such dynamic behaviors correctly. Therefore, precise numerical algorithms are used for the time integration of atomic motions. Among these algorithms, integration techniques that strike a compromise between computational accuracy and efficiency play a pivotal role in the reliable prediction of particle trajectories. The velocity-Verlet algorithm provides an excellent illustration, successfully updating particle positions and velocities while simultaneously preserving numerical stability through consideration of interaction and integration over time [22-24]:

$$r_i(t+\Delta t) = 2\, r_i(t) - r_i(t-\Delta t) + \left(\frac{d^2 r_i}{dt^2}\right)(\Delta t)^2 \quad (2)$$

$$v(t+\Delta t) = v(t) + \Delta t\, v(t) + \frac{\Delta t\left(a(t)+a(t+\Delta t)\right)}{2} \quad (3)$$

In MD simulations, accurately defining how each particle interacts is critical for predicting its trajectory and other time-related behavior. The interaction potential serves as a mathematical construct that describes forces acting among atoms or molecules in the system. The model mentioned encompasses attraction and repulsion due to electrical charges, short-range dispersive effects, and, of course, forces of chemical bonding. An accurate evaluation of these forces allows any simulation to reproduce realistic physical dynamics in a virtual environment [25].

$$E_{total} = E_{bonded} + E_{nonbonded} \quad (4)$$

There is a need for models of sufficiently high theory to describe fundamental interaction forces that control the interaction among the particles inside molecular frameworks. Such models would include potential energy functions, of which LJ potentials and Coulomb potentials frequently find use while determining interparticle forces [26-29]. The LJ potential is invaluable in MD simulations as it expresses in mathematical terms the state of balance of repulsive with attractive forces as experienced by a neutral atom or a molecule as a function of the intermolecular distance. It is the repulsive contribution that is responsible for repulsion on account of the Pauli exclusion principle-which resists diffuse overlap of digitized electron clouds of the two atoms-and the attractive contribution is due to London dispersion forces, which can cause weak long-range attractions. With those two components at work, such potential functions have offered a very critical understanding of energetic landscapes governing molecular behavior in order to facilitate better characterization of aggregation, phase transition, and molecular conformations [30].

$$U_{LJ} = 4\varepsilon\left[\left(\frac{\sigma}{r}\right)^{12} - \left(\frac{\sigma}{r}\right)^{6}\right] \qquad r < r_c \quad (5)$$

These two parameters, ε and σ, are fundamental for the quantitative characterization of intermolecular interactions at the atomic level. The parameter ε is understood to represent the depth of the potential well, thus providing a measure of

the strength of attraction IE among particles. The IE between the asphaltene molecules and the lime NPs was calculated in LAMMPS using the 'compute group/group command'[31]. This computation includes LJ and Coulombic nonbonded interactions between two groups, with long-range electrostatics treated using PPPM solver. The obtained IE thus showed the net asphaltene–NP interfacial IE. In contrast, σ defines the finite distance at which interparticle potential energy becomes zero, effectively representing the collision diameter or the range of repulsive interactions [32, 33].

$$\varepsilon_{ij} = \sqrt{\varepsilon_i \varepsilon_j} \tag{6}$$

$$\sigma_{ij} = \frac{\sigma_i + \sigma_j}{2} \tag{7}$$

In electrostatic potential energy, one defines the energy stored in a system of electric charges due to their spatial arrangement and mutual interaction. This potential energy, being based on the electrostatic principles, depends on the magnitude of each charge and the distances separating them from one another. The proportionality constant that governs the interaction strength represents the medium in which the charges reside. The total energy of the system is computed as a sum of pairwise interactions among all charges with consideration of their relative positions. The accurate assessment of this energy plays a vital role in comprehending phenomena ranging from atomic-scale interactions to macroscopic electrical behavior in complex systems [26]:

$$U_{ij}(r) = \frac{-1}{4\pi\varepsilon_0} \frac{q_i q_j}{r_{ij}^2} \tag{8}$$

2.1. Present simulation details

Asphaltene precipitation and surface adsorption are critical impacts in the petroleum and environmental areas, greatly affecting reservoir permeability and pipeline fouling, along with separation processes. Hence, MD simulations were used to investigate the adsorption behavior of asphaltene molecules on lime-based NPs and in the presence or absence of water. The simulations were run on the LAMMPS software package [34] with a cubic SB measuring 150 cubic blocks 150 × 150 × 150 Å³. The asphaltenes consisted of a complex mixture of molecules that were quite heterogeneous, but perhaps not the worst possible scenarios. Generally speaking, asphaltenes were high molecular weight polyaromatic compounds with heteroatoms associated with N, O, and maybe S that imparted considerable polarity to these molecules. In this study, the most widely used asphaltene structure, M1, was employed. Asphaltene M1 contained 5 aromatic rings and two methyl groups. The asphaltene structure is modeled by Avogadro software with the formula $C_{65}S_2N$. This designed structure is optimized with the Conjugate Gradient (CG) method. In the subsequent step, water molecules were introduced as a solvent to evaluate the influence of hydration on the adsorption process. Both water and NP models were constructed using Avogadro and combined into a unified system via the Packmol software. Asphaltene molecules were modeled as representative polycyclic aromatic structures with nitrogen, oxygen, and sulfur heteroatoms that were characteristic of actual asphaltenes. Multiple aromatic rings and functional groups were included in these M1-type asphaltene models, representing the key structural and polar features required to study the adsorption behavior. Molecular geometries were optimized in Avogadro before combining water and NP models using Packmol for a realistic initial configuration in MD simulations [35, 36]. Calcite and dolomite NPs were inserted into the silica bead (SB) using the Packmol package. Periodic boundary conditions were applied to avoid any edge effects in all three spatial directions. After the construction of the structure, an energy minimization was performed using a steepest descent method for 100,000 time steps to remove any initial configurations that were unfavorable to the buildup. Initially, the system was equilibrated in the microcanonical (NVE) ensemble, after which it switched to the canonical (NVT) ensemble to stabilize T and equilibrate the system. The equilibrium was determined by monitoring thermodynamic properties like system T and KE. Once equilibrium was reached, properties, such as the number of asphaltene molecules adsorbed, density profiles, and interaction energies (IEs) were calculated. A Nosé–Hoover thermostat was used to control T during the entire simulation. A time step of 1 fs was employed throughout the production simulations, while sampling was conducted every 10,000 steps for analyzing the adsorption behavior. The atomic model for the initial configuration is depicted in Fig. 1. The simulated system consisted of approximately 38,200 atoms contained within

a 150 Å SB. The system is composed of 20 wt% calcite NPs relative to the asphaltene mass. MD simulation settings are presented in Table 1. The choice of lime ($CaCO_3$) NPs and a relatively high loading of approximately 20 wt% was motivated by previous studies demonstrating the effectiveness of calcium-based NPs in mitigating asphaltene aggregation under reservoir-relevant conditions [16]. In particular, Shadervan et al. [16] reported that even at low concentrations, $CaCO_3$ NPs can significantly inhibit asphaltene precipitation and improve dispersion stability in crude oil systems. Thus, with the present study applying a higher NP loading, molecular-level interactions and their adsorption mechanisms were studied more comprehensively by MD simulations, which in turn provided insight into the presumably maximum adsorption efficiency and T-dependent behavior of asphaltene-lime NP systems.

3. Equilibration Process

Temp profile of the simulated system over a 10-ns equilibration period at a target T of 300 K is shown in Fig. 2. At the very beginning of the simulation, large fluctuations in T were observed, which were normal and mainly caused by the random assignment of initial atomic velocities and the non-equilibrium conditions during the thermalization phase. As time progressed with the simulation, the stabilization of the system occurred gradually, and T started to converge towards the target value. The preparation with a 10 ns equilibration time and a 10 ns production run guaranteed thermal stability and sufficient sampling of the adsorption events in the asphaltene-lime NP system. During the equilibration process, we found that T, total energy, and kinetic energy were monitored to converge towards a steady value, thus confirming that the system was in a stable condition and able

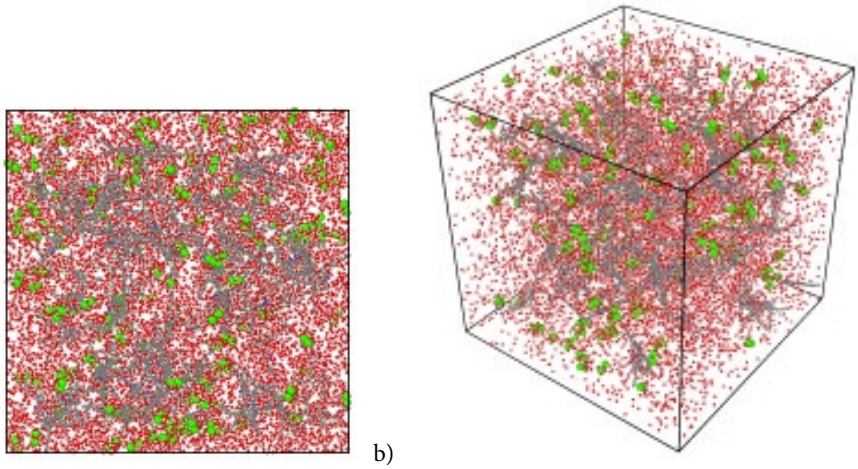

Fig. 1. Atomic structure modeled in the present study in the initial step of MD simulation from side and perspective views.

Table 1. MD simulation settings in current research

Computational Parameter	Parameter Ratio/Setting
Simulation software	LAMMPS
Molecular Builder Editor	Avogadro/ Packmol
MD Box Size	150×150×150 $Å^3$
Number of atoms	38,200
NP content	20 wt%
Time step	0.1 fs
Ensemble	NVE/NVT
Equilibration time	10 ns
Force field	LJ & Coulomb
Thermostat	Nosé–Hoover
Energy minimization	100,000 steps cg

to produce simulations. Earlier MD studies on asphaltene adsorption on NPs and mineral surfaces suggested that for small to medium system sizes (~30,000–50,000 atoms), equilibration times in the range of 5–15 ns would usually be enough to achieve thermal and structural equilibrium [37-39]. Adsorption events in such systems usually take a few nanoseconds as molecules diffuse and attach to NP surfaces. In these simulations, around 69% of asphaltene molecules adsorbed during the first 7 ns, showing that the selected timescale can capture the majority of adsorption events; thus, the subsequent 10 ns production run provided for good sampling to compute density profiles, radial distribution functions, interaction energies, and adsorption kinetics with statistical certainty. Thus, T changed around the 299.44K mark by the conclusion of the equilibration period; the deviation from the desired T was nevertheless very less, that is, about 1K, thus evidencing good thermal stability and equilibration efficacy. Given a physical understanding, this behavior means that the translational KE was evenly distributed among all atoms, and T fluctuations were reduced.

With the average KE of the atomic system at equilibration fluctuating (Fig. 3), a convergence point where KE stabilizes was reached at approximately 0.86 kcal/mol and continued well with the T convergence displayed in Fig. 2. This consistency confirmed that the thermal equilibration was done properly. From a physical point of view, looking at those few nanoseconds reveals restrictions in atomic motions around their equilibrium positions, and thus a continuous decline in KE fluctuations. That is actually a gradual decrease in amplitude for atomic oscillations and establishment of a dynamically stable state in MD terms.

4. Redial Distribution Function (RDF)

Besides visual inspection of molecular configurations, quantitative structural analysis was required for a full comprehension of asphaltene behavior in the simulated system. One of the most useful tools for structural analysis was the radial distribution function (RDF): it outlined the detailed coexistence of molecules from the spatial view by describing how the density of a particle varied with distance from a reference particle. RDF was calculated among asphaltene molecules in the SB after confirming that the system attained thermodynamic equilibrium. In the analysis shown in Fig. 4, there were many well-defined peaks appearing at specific radial distances. The peaks were indicative of short-range ordering within the asphaltene structure, that is, some intermolecular distances were statistically favored over others. The first prominent peak usually showed either the most probable or the equilibrium distance among the centers of mass of neighboring

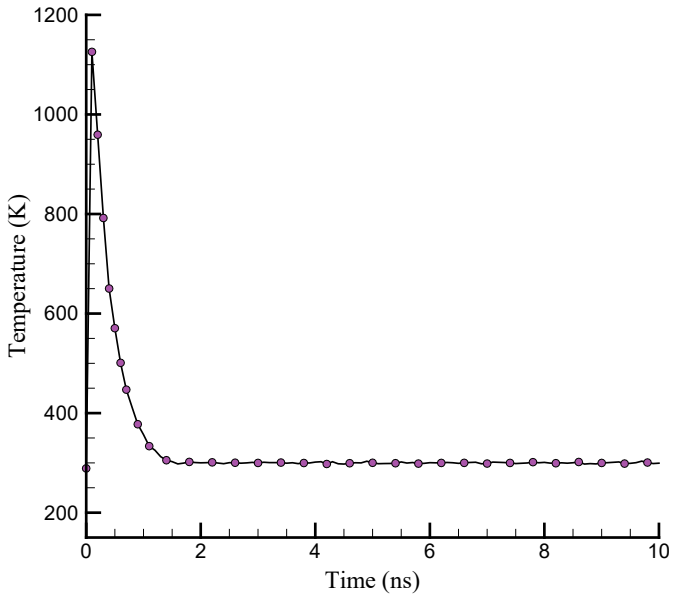

Fig. 2. T changes over simulation time in the atomic structure during the equilibration stage at an initial T of 300 K.

asphaltene molecules. The presence of these peaks and their periodicity agreed with values from earlier numerical and experimental studies, thus corroborating the structural soundness of the model and its simulation parameters, such as force field, T, pressure, and integration scheme. The shape and characteristics of RDF were consistent with average packing and statistical distribution of asphaltene molecules in the system. Thus, a very good match of simulations with experimental results validated the simulation approach adopted in the present study [40]. This structural validation resulted from suitable atomic modeling and MD settings (e.g., force field, time-step, etc) in chosen conditions and a validated current method to describe their atomic performance. In addition, this correlation

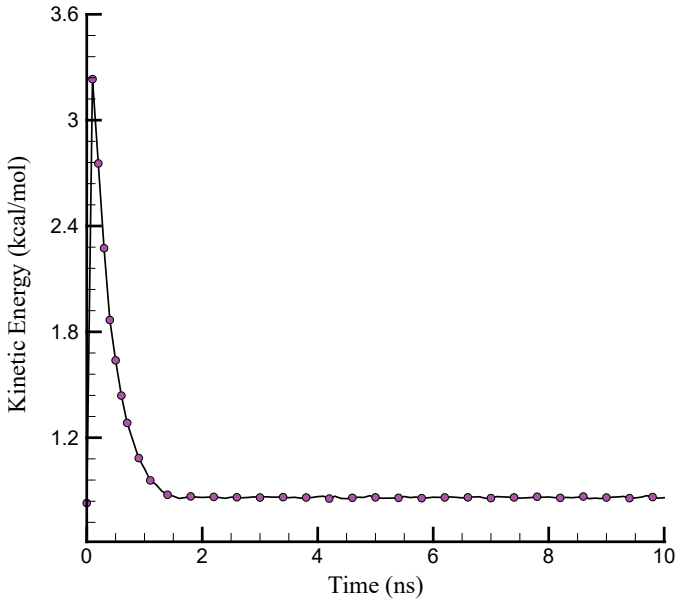

Fig. 3. KE changes versus simulation time in the atomic structure during the equilibration stage at an initial T of 300 K.

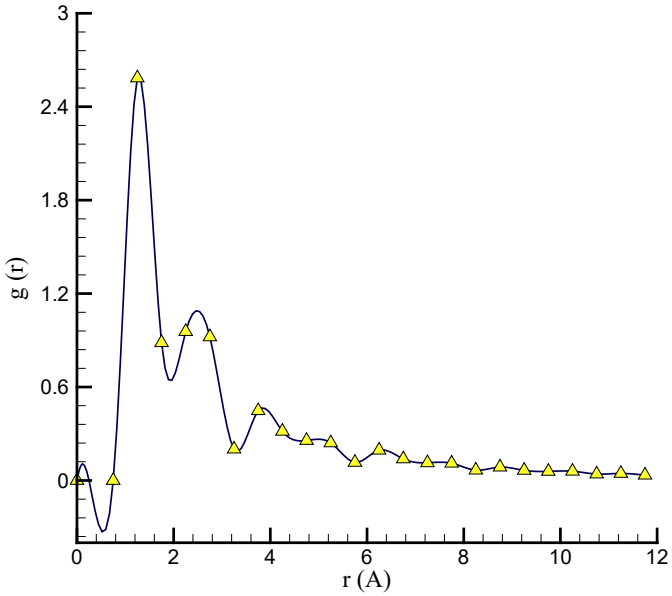

Fig. 4. Overall RDF of the asphaltene structure after observing thermodynamic equilibrium at 300 K.

demonstrated that the model can reliably capture the temporal evolution and structural stability of asphaltene aggregates.

5. Results and discussion

5.1. Atomic behavior of the primary structure

The current study undertook an extensive understanding of the asphaltene and lime NP system by evaluating multiple descriptors, such as density profiles, RDFs, ionization energy, and adsorption kinetics of varied Ts. Moreover, multi-aspect evaluation through MD simulated analysis of density profiles, RDFs, interaction energies, and adsorption kinetics was performed for all asphaltene molecules on lime NPs. Density profiles revealed that asphaltene tended to be located around NPs preferentially, while RDF analysis exhibited some evidence for short-range ordering and structural stability, confirming the previous literature. Interaction energy was noted to increase due to adsorption, reflecting the improvement in molecular binding, while adsorption kinetics demonstrated that ~69% of molecules adsorbed within the first 7 ns, thereafter reaching a saturation plateau. T-dependent simulations further confirmed that at higher thermal conditions, NP-asphaltene interaction decreased, thereby presenting an evaporative local density and less optimum adsorption efficiency at 350 K, which reduced to below about 56%. Such outputs would translate into a very detailed quantitative insight regarding nanoscale adsorption mechanisms, thus taking into account the engineering of T-stable nanofluid systems for asphaltene mitigation concerning T effects. Upon validation of the thermodynamic equilibrium in the atomic system, the adsorption of asphaltene molecules on lime NPs was rigorously studied. Important output

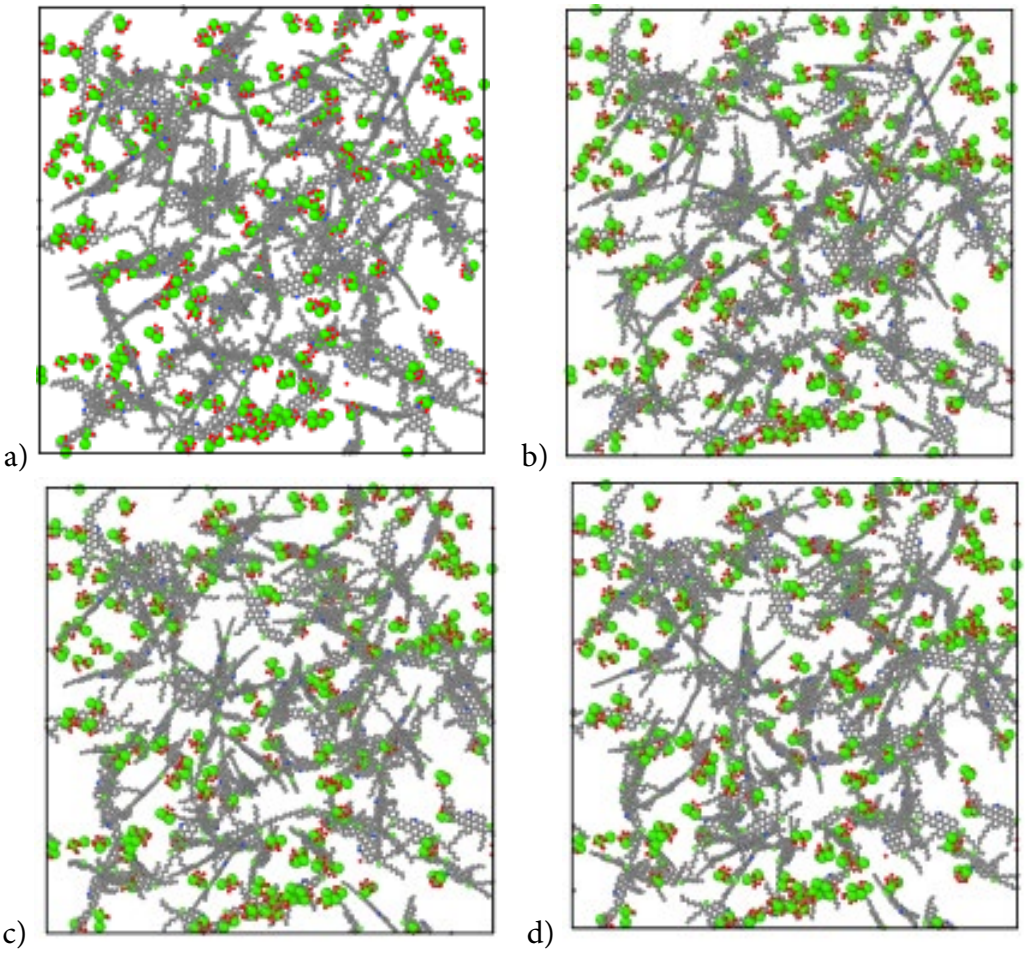

Fig. 5. Structural changes of the simulated atomic sample in the final asphaltene-lime NP adsorption process.

parameters, such as the density profile, the IE, and the adsorption efficiency, were calculated and discussed. The atomic configuration of the encoded system in Fig. 5 represents the system's structural evolution throughout the adsorption phase. The figure depicts the dynamic traveling of the molecular arrangement, confirming the stable structure of the simulated model over adsorption.

In order to fully understand the spatial arrangement of asphaltene molecules and develop a mechanistic understanding of the adsorption of asphaltene molecules onto lime NP surfaces, it was necessary to analyze the molecular density profile along with SB coordinates. Therefore, after the completion of the adsorption process, the atomic density profile of the system was calculated and is shown in Fig. 6. This profile showed the average atomic density distribution with a focus on the localization of asphaltene molecules within the simulation domain. It is clear that the density peaks at the middle of the SB, reaching maximum atomic density at about 180.72 atom/Å3. This distribution indicated that asphaltene molecules preferentially adsorbed around the lime NPs that were initially deposited at the center of SB. In other words, in the light of physicochemical characteristics, this was explained by strong interactions among the polar functional groups of asphaltene molecules and the chemically active surface sites of lime NPs, which favored aggregation and localization of molecules, thereby driving them toward further ordering near the NP surface.

Fig. 7 provides the temporal profile of IE between lime NPs and asphaltene molecules during the adsorption simulation. In MD studies, the IE was an important descriptor of physical and chemical affinities among components, since it considers the cumulative influence of van der Waals forces, electrostatic interactions, and other surface-specific binding mechanisms. The simulation data showed a steady rise in IE over time and reached a maximum value of ~0.047 kcal/mol after 10 ns. This therefore suggested a continuous adsorption of asphaltene molecules on the NP surface over time. Hence, with increasing proximity of the molecules, the interfacial interactions are increasingly pronounced, leading to higher attractive energy with higher IE. So, an observed increase in IE correlated with a smaller intermolecular distance and a greater number of adsorbed molecules at the solid–liquid interface. Mechanistically, this trend signified the progressive system relaxation as asphaltene molecules approached energetically favorable adsorption sites on the lime NP surface. The plateau at the end of the simulation indicated equilibrium conditions in this particular system, with small fluctuations of IE, indicating the completion of the adsorption process and formation of a thermodynamically stable configuration.

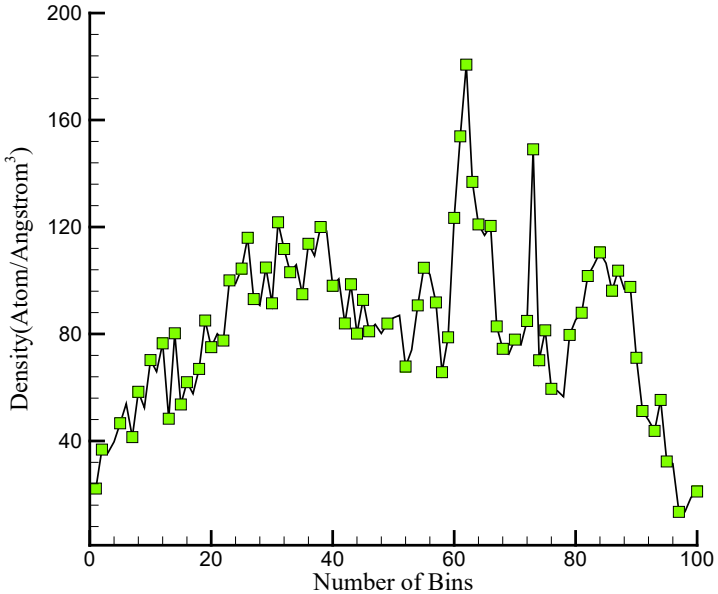

Fig. 6. Simulated atomic sample density profile in the final adsorption process.

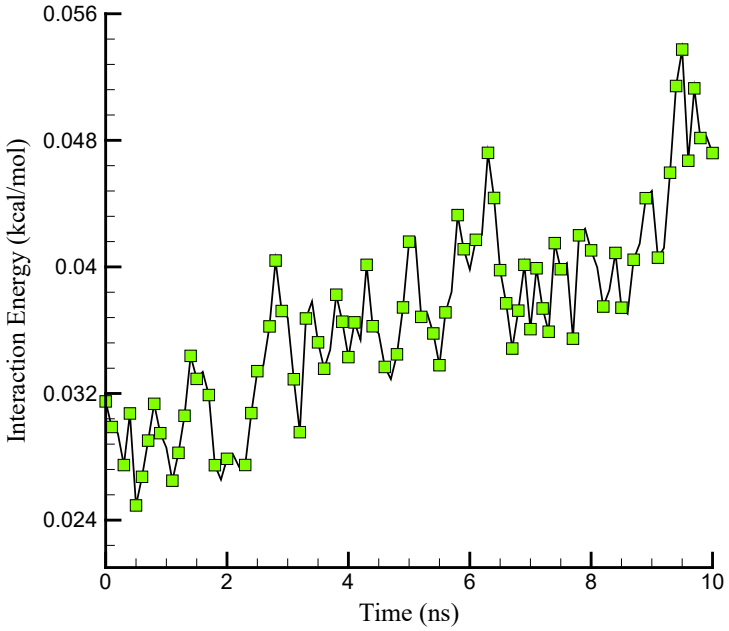

Fig. 7. Time variations of the IE between lime NPs and asphaltene molecules in the final adsorption process.

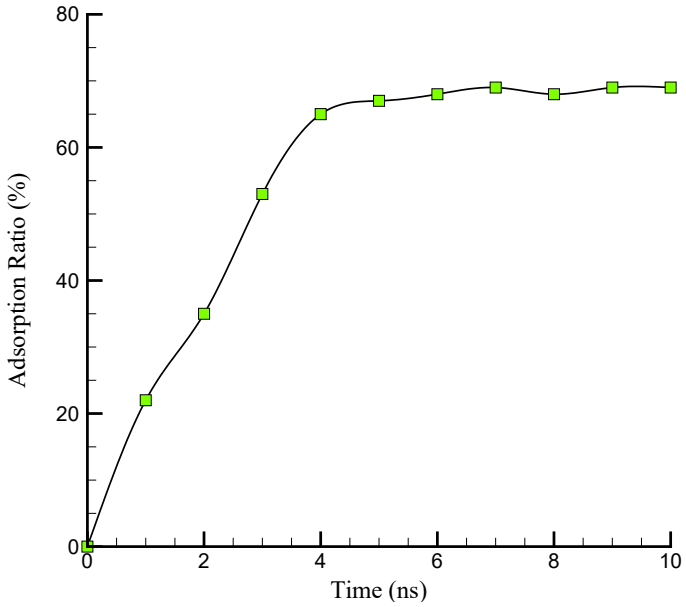

Fig. 8. Time changes in the adsorption amount between lime NPs and asphaltene molecules in the final adsorption process.

The evaluation of the adsorption of asphaltene molecules against lime NPs was carried out qualitatively by carrying out an atomic-scale structural analysis. The functional criterion for classification of the NPs adsorbed or not adsorbed was based on including NPs found at a distance of up to 5 Å away from the asphaltene molecules. Events on the temporal development of adsorption percentage are exhibited in Fig. 8. Initial data indicated that most of the adsorption takes place over the first 7ns; after this time, the process entered a phase approaching a saturation plateau. At the end of the simulation, the adsorption percentage remained approximately 69%, clearly confirming the effective capacity of lime NPs for adsorbed asphaltene molecules in the system. This trend

indicated both practically that thermodynamic equilibrium was ultimately achieved and that all available active sites were now fully occupied on NP surfaces. After this point, they were rendered due to the limited availability of adsorbing sites, showing diminished propensity for further adsorption, with only small variations reflecting thermal vibrations and local rearrangement of atoms at the interface.

5.2. T effect

The variations of T and pressure brought about a change in the initial conditions of the simulated sample. In this first stage of the current stage, T changes were considered, and these were equal to 300, 310, 325, and 350 K. In Fig. 9, it is observed that the NP-asphaltene system was structurally stable in all samples. Among all previous studies on NP type or concentration, not much research has been carried out on thermal fluctuations and their effects on adsorption efficiency, strength of interactions, and molecular arrangement. These simulations demonstrated that with an increase in T, the asphaltene-lime NP was weakened and had lowered surface coverage, which was consistent with the previous MD results on asphaltene aggregation with T changes [41, 42]. It contributed to a fundamental understanding of binding at the nanoscale under thermal stress, providing actual conditions for T-stabilized nanofluids on asphaltene reduction design. This trend resulted from the limitation of the oscillation range of atoms and the dominance of the interatomic attractive force over the mobility of atoms.

Increasing the initial T of the system affected the spatial distribution of the molecules (Fig. 10). Looking at the output of the simulation, it can be said that with an increase in the T of the system, the maximum value of density decreased. From a physical point of view, this behavior was due to the direct influence of heat on the KE of molecules,

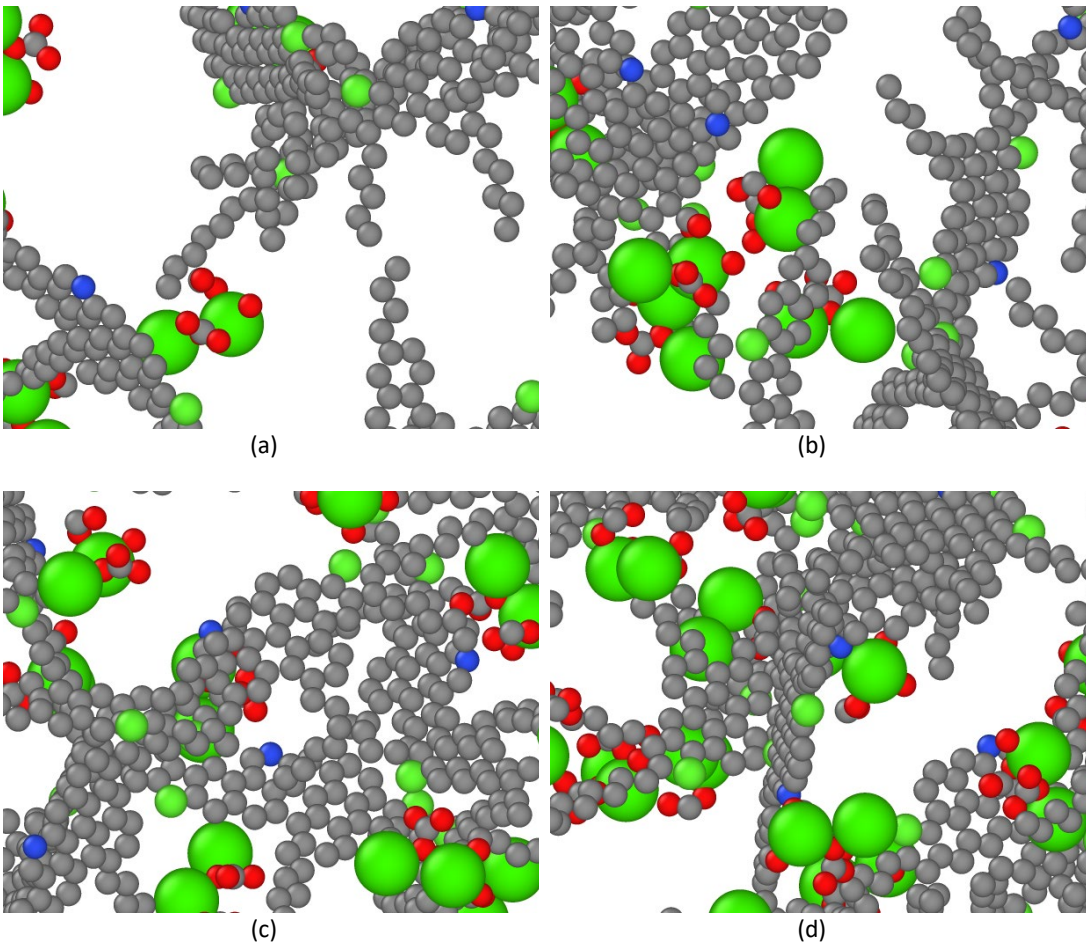

Fig. 9. Time evolution of lime NPs and asphaltene molecules at initial Ts of a) 300, b) 310, c) 325, and d) 350 K.

with the result that at higher Ts the particles were allowed to move more freely in space. More KE gave them a wider oscillatory range, and as such, the asphaltene molecules, along with other components of the system, start spreading fast in various regions of SB. Consequently, the local density of particles diminished, and they became more widely distributed. However, the center of the system remained the dominant region of particle aggregation, indicating that the intermolecular attractive forces had not completely disappeared and retained their effect.

Fig. 11 represents the trends of interaction energy (IE) changes between lime NPs and the asphaltene molecules at various Ts. The simulation results indicated that upon raising the initial T of the system from 300 to 350 K, the value of IE decreased from 0.047 to 0.031 kcal/mol, suggesting weakness in the intermolecular interactions and thereby less stability of the adsorbed structure. Physically, T increase increased the kinetic energy of the particles within the system and increased mobility, especially for the asphaltene molecules. The increase in mobility of the asphaltene molecules

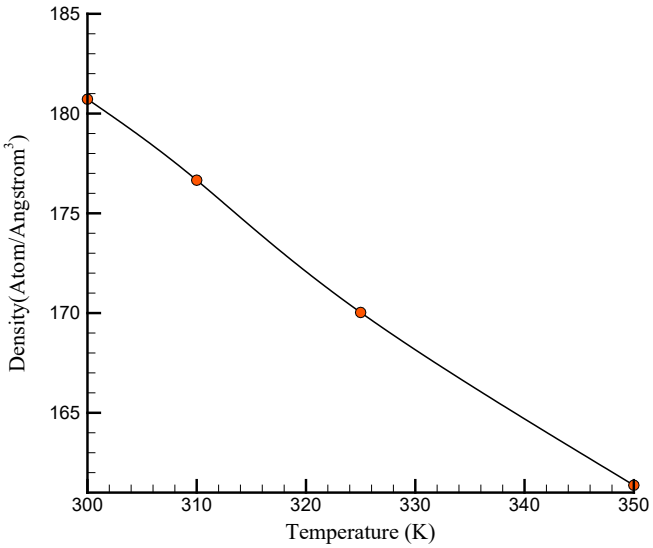

Fig. 10. Changes in maximum density depending on T.

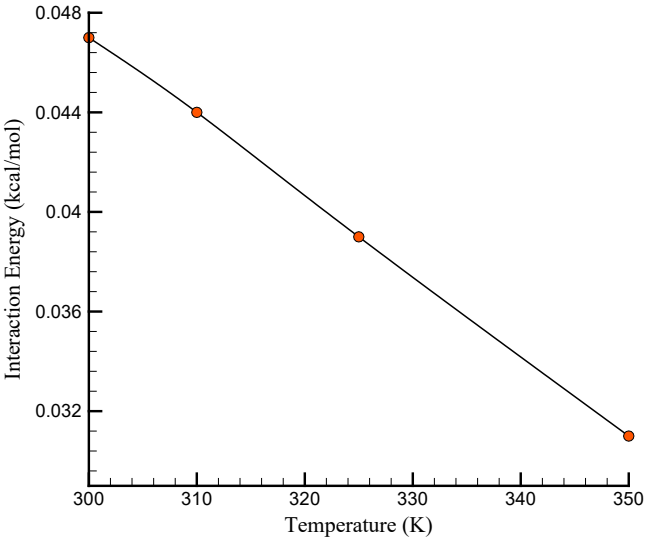

Fig. 11. Changes in NPs-asphaltine IE depending on T.

translated to increased inter-particle distances at the nanoscale and a decrease in effective contact time between the NP surface and the asphaltene molecules. Effectively, the decrease in IE noted in the computational box could indicate that the process of adsorption of asphaltene molecules became less efficient, which was suggested by previous experimental investigations already [37, 43, 44]. The agreement between these earlier reports and the current MD outputs gave credence to the simulation approach employed in the study, and numerical/physical outputs of such simulations (with defined settings) should be regarded with reference to their real-life applications.

For instance, the figure showed the changes related to the percentage of adsorption of asphaltene molecules due to lime NPs, which changes with T. Simulated results showed the final adsorption percentage reduced from 69 to 56% when T increased from 300 to 350K. This decline in the final percentage of adsorption was indicative of the lower efficiency of the system at higher Ts. The increased T caused further thermal motion and disorder, inducing spatial disorder among asphaltene molecules inside the SB. This increased mobility led them to move more about the free space of the box instead of clustering around the adsorbent surface. This reduced the probability of effective placement near the active surface of NPs, and weakened, therefore, the trapping process by the surface. Such analysis indicated that the final effectiveness of lime NPs in effective adsorption of asphaltene molecules depended directly on the thermodynamic conditions existing in the system, including its initial T, and hence should be carefully considered in the practical design of nanosorbent systems. The analysis of simulated results was meaningful for lime NPs' use in asphaltene mitigation in real life. In the analysis of the temperate case, it was evident that adsorption efficiency reduced from 69% at 300 K down to 56% at 350 K, thus showing the significant effect of thermal conditions on the effective binding of asphaltene molecules. This consequently indicated the extreme importance of controlling operational Ts within industrial processes, such as crude oil treatment and pipeline maintenance, so as to achieve optimum performance of nanosorbent systems. Increased Ts reduced adsorption efficiency; however, the framework stability of the NP-asphaltene system seemed ultimately preserved. This indicated that functional integrity under moderate thermal stress could be retained by lime NPs, which can form a good selection for industrial environments with frequent T fluctuations. The observed interactions between polar functional groups of asphaltene molecules and the chemically active NP surfaces further suggest that surface engineering of NPs might enhance adsorption under even less favorable thermal conditions, in agreement with previous MD and experimental studies on T effects on asphaltene aggregation and adsorption [45, 46]. Moreover, the detailed data analysis-including density profiles, radial distribution functions,

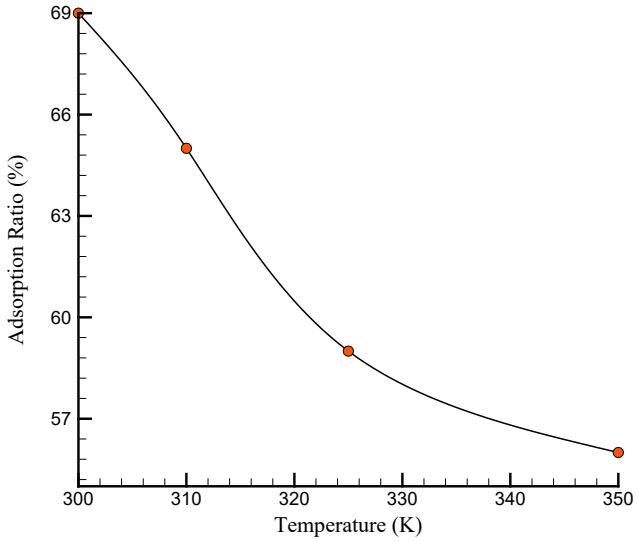

Fig. 12. Changes in the percentage of adsorption in the NP-asphaltene system depending on T.

interaction energies, and adsorption kinetics, gave a mechanistic understanding of the adsorption process. For example, the density profiles suggested preferential aggregation of asphaltene near NP surfaces, while the trends in the IEs correlated directly with adsorption strength and molecular mobility [46]. Such insights can guide the rational design of nanosorbent systems by enabling the selection of particle size, surface chemistry, and operating conditions that maximize adsorption and stability. In summary, the present study advanced not only the fundamental understanding of nanoscale interactions under varying thermal conditions but also offered practical guidance toward the development of T-stable nanofluids and nanosorbent systems for asphaltene control in petroleum-related applications. Such inferences can be used directly in the optimization of treatment strategies, which would enhance operational efficiency and decrease the risk of fouling or deposition in the industrial part [47].

Table 2 presents the relationship between physical quantities governing the adsorption of asphaltene in the presence of lime NPs at varying initial Ts. With an increase in initial T from 300 to 350 K, the maximum density, IE between the NP and asphaltene, and adsorption percentage decreased. This trend thus confirmed that increasing T had an adverse effect on the efficiency of the adsorption process. Physically, increasing T resulted in increased KE of the molecules [48], thus reducing the effective contact time with the NP surface. Hence, a decrease in the adsorption rate would imply weaker molecular interactions between asphaltene and the adsorbent surface. The continuous decrease in IE and density profile strengthened the argument for a decrease in the stability of higher-T adsorbed structure concentration. Thus, these findings emphasized that the selection of T was an important consideration in the design and optimization of any nanosorbent systems.

The seemingly small changes in physical parameters with T were collected and reviewed in a tabular arrangement for quick comparison with all T-dependent variations shown in the simulations: density distribution near the NP surface, adsorption kinetics, adsorption efficiency, and structural stability. Table 3 shows how T influenced the molecular packing, interaction strength, and adsorption performance of asphaltene onto lime NPs. Thus, extracted values hindered direct comparison among different thermal conditions and presented a clearer view of the fundamental mechanisms that controlled the adsorption process.

Table 2. Physical outputs obtained for the target atomic sample in terms of the percentage of lime NPs inside the SB

T (K)	Maximum density (atom/Å^3)	NP-asphaltene IE (kcal/mol)	Adsorption Ratio (%)
300	180.72	0.047	69
310	176.66	0.044	65
325	170.03	0.039	59
350	161.37	0.031	56

Table 3. Summary of key physical outputs at different Ts based on MD simulation

Property/outcome	Value at 300 k	Value at 350 k	Interpretation
Adsorption efficiency (%)	69%	56%	Higher T weakens intermolecular interactions.
IE (kcal/mol)	0.047	0.031	Adsorption becomes less energetically favorable at higher Ts.
Maximum atomic density (atoms/Å^3)	180.72	161.37	Reduction caused by thermal expansion; weaker molecular packing at higher T.
Time to reach adsorption saturation	7 ns	Higher than 7 ns	Increased molecular mobility at higher T slows down adsorption kinetics.
Structural stability	Stable configuration maintained	Slightly reduced structural ordering	Consistent with lower IE at higher T.

6. Limitations of the MD Simulation and Future Research Directions

With precious molecular-level insight for asphaltene adsorption onto lime NPs, this study left much to be desired. The SB size is finite, which may still exert a pull on the particle behavior; an attempt is being made to fix it by periodically considering the box. This assumption disregarded gravity and holds that the structure was ideal. The simulations were conducted under a really simple aqueous environment, which did not capture the intricacies of crude oil systems, and the timescale may not be adequate to capture the long-term dynamics of adsorption. Additionally, surface functionalization effects of NPs, the polydispersity of asphaltene molecules, and the influence of different solvent compositions were not examined. Future research may overcome these limitations using larger and more realistic SBs, multi-component oil environments, functionalized or mixed NPs, longer simulation times, and an integration of molecular simulations with experimental studies to inform industrial applications and optimize nanofluid formulations.

7. Conclusion

The adsorption behavior of asphaltene molecules onto lime NPs was investigated through computational simulations. In this regard, MD simulations for 20 ns were carried out using the LAMMPS software package. In the first 10 ns, atomic models consisting of asphaltene molecules and 20% lime NPs in an aqueous environment were equilibrated. After equilibration, the structural adsorption process was studied. The main results obtained during the equilibration phase are summarized as follows:

- The mobility of the defined atomic system decreased after 10 ns, indicating that the system had reached thermodynamic equilibrium and structural stability within SB.
- T and KE converged to approximately 299.44 K and 0.86 kcal/mol, respectively, confirming the thermodynamic equilibrium of the system.
- Subsequently, the adsorption process was simulated for an additional 10 ns in the NP-asphaltene system, yielding the following results:
- A significant adsorption of asphaltene molecules was observed, with the maximum atomic density reaching approximately 180.72 atoms/Å^3 at the center of SB, suggesting strong localization around lime NPs.
- The IE between each asphaltene molecule and the lime NPs gradually increased to around 0.047 kcal/mol over 10 ns, indicating progressive adsorption and eventual thermodynamic stabilization.
- According to the adsorption analysis, approximately 69% of the asphaltene molecules were adsorbed onto NP surfaces in the first 7 ns, after which the process reached saturation, demonstrating efficient adsorption and equilibrium.
- A rise of an initial T of 300 K to 350 K resulted in a decrease in maximum atomic density, from 180.72 down to 161.37 atoms/Å^3, signifying a molecular structure that was less dense, but more uniformly distributed.
- Surface Adsorption Energy (IE) diminished from 0.047 to 0.031 kcal/mol when T rose from 300 K to 350 K, which indicates weakened molecular interactions of lime NPs with asphaltene molecules and a more compact overall arrangement of them.
- The asphaltene adsorption ratio decreased from 69% to 56% with the increase in T, which further indicated a decrease in the adsorption potential available to the asphaltenes for lime NPs and a tendency toward a more compact structural organization.

Funding declaration

No funding was received for conducting this study.

Declaration of competing interest

The authors declare that they have no known competing financial interests or personal relationships that could have appeared to influence the work reported in this paper.

Nomenclature

Nanoparticle	NP
Molecular Dynamics	MD
Lennard-Jones	LJ
Interaction Energy	IE
kinetic energy	KE
Redial Distribution Function	RDF
Simulation Box	SB
Constant Number, Volume, Energy ensemble	NVE
Constant Number, Volume, Temperature ensemble	NVT
Particle–Particle Particle–Mesh	PPPM

References

[1] S. Alimohammadi, S. Zendehboudi, L. James, A comprehensive review of asphaltene deposition in petroleum reservoirs: Theory, challenges, and tips, Fuel 252 (2019) 753–791. https://doi.org/10.1016/j.fuel.2019.03.016

[2] S. Kashefi, M.N. Lotfollahi, A. Shahrabadi, Investigation of asphaltene adsorption onto zeolite beta nanoparticles to reduce asphaltene deposition in a silica sand pack, Oil Gas Sci. Technol.–Rev. IFP Energies Nouv. 73 (2018) 2. https://doi.org/10.2516/ogst/2017038

[3] G. Raj, E. Larkin, A. Lesimple, P. Commins, J. Whelan, P.E. Naumov, In situ monitoring of the inhibition of asphaltene adsorption by a surfactant on carbon steel surface, Energy Fuels 33 (2019) 2030–2036. https://doi.org/10.1021/acs.energyfuels.8b04246

[4] J. Taheri-Shakib, M. Rajabi-Kochi, E. Kazemzadeh, H. Naderi, Y. Salimidelshad, M.R. Esfahani, A comprehensive study of asphaltene fractionation based on adsorption onto calcite, dolomite and sandstone, J. Pet. Sci. Eng. 171 (2018) 863–878. https://doi.org/10.1016/j.petrol.2018.08.024

[5] S. Alafnan, Asphaltene behavior during thermal recovery: A molecular study based on realistic structures, Minerals 12 (2022) 1315. https://doi.org/10.3390/min12101315

[6] S. Yang, C. Yan, J. Cai, Y. Pan, Q. Han, Research progress in nanoparticle inhibitors for crude oil asphaltene deposition, Molecules 29 (2024) 1135. https://doi.org/10.3390/molecules29051135

[7] A.D. Manasrah, T. Montoya, A. Hassan, N.N. Nassar, Nanoparticles as adsorbents for asphaltenes, in: Nanoparticles: An Emerging Technology for Oil Production and Processing Applications, Springer, 2022, pp. 97–129. https://doi.org/10.1007/978-3-319-12051-5_3

[8] A. Talebi, M. Shafiei, Y. Kazemzadeh, M. Escrochi, M. Riazi, Asphaltene prevention and treatment by using nanomaterial: A comprehensive review, J. Mol. Liq. 382 (2023) 121891. https://doi.org/10.1016/j.molliq.2023.121891

[9] A. Solaimany Nazar, F. Amin, A study on the adsorption and catalytic oxidation of asphaltene onto nanoparticles, J. Pet. Sci. Technol. 7 (2017) 21–29. https://jpst.ripi.ir/article_745.html

[10] M. Madhi, A. Bemani, A. Daryasafar, M.R. Khosravi Nikou, Experimental and modeling studies of the effects of different nanoparticles on asphaltene adsorption, Pet. Sci. Technol. 35 (2017) 242–248. https://doi.org/10.1080/10916466.2016.1255641

[11] C.A. Franco, N.N. Nassar, M.A. Ruiz, P. Pereira-Almao, F.B. Cortés, Nanoparticles for inhibition of asphaltenes damage: Adsorption study and displacement test on porous media, Energy Fuels 27 (2013) 2899–2907. https://doi.org/10.1021/ef4000825

[12] M. Baninaam, S.A. Hosseini, A.R. Abbasian, Isothermal study of asphaltene adsorption over 4A, 13X, ZSM-5, clinoptilolite zeolites, and phoslock, Appl. Petrochem. Res. 10 (2020) 49–54. https://doi.org/10.1007/s13203-020-00243-x

[13] M.S. Mazloom, A. Hemmati-Sarapardeh, M.M. Husein, H.S. Behbahani, S. Zendehboudi, Application of nanoparticles for asphaltenes adsorption and oxidation: A critical review of challenges and recent progress, Fuel 279 (2020) 117763. https://doi.org/10.1016/j.fuel.2020.117763

[14] B. Zhu, et al., Insights into the effect of water content on asphaltene aggregation behavior and crude oil rheology: A molecular dynamics simulation study, J. Mol. Liq. 396 (2024) 124042. https://doi.org/10.1016/j.molliq.2024.124042

[15] T. Lu, Z. Li, L. Du, Enhancing foam stability and addressing asphaltene deposition for improved oil recovery in CCUS applications using aerogel nanoparticles, Chem. Eng. J. 481 (2024) 148290. https://doi.org/10.1016/j.cej.2023.148290

[16] A. Shadervan, A. Jafari, A. Teimouri, R. Gharibshahi, A.H.S. Dehaghani, Mechanistic understanding of asphaltene precipitation and oil recovery enhancement using SiO2 and CaCO3 nano-inhibitors, Sci. Rep. 14 (2024) 15249. https://doi.org/10.1038/s41598-024-65995-1

[17] M.R. Torki, M. Rahimi, M. Hekmatifar, Use of Fe3O4 nanoparticles for adsorption of asphaltene from heavy and ultra-heavy materials: A molecular dynamics study. https://cnj.araku.ac.ir/article_723508.html

[18] N. Hayatizadeh, F.F. Chanzab, C. Falamaki, Adsorption of asphaltene molecules on functionalized SiO2 nanoparticles at atmospheric and high pressures in heptane/toluene environment: A molecular dynamics simulation study, Geoenergy Sci. Eng. 234 (2024) 212684. https://doi.org/10.1016/j.geoen.2024.212684

[19] A.S. Al Qasim, Simulation of asphaltene deposition during CO_2 flooding, 2011.

[20] C. Huang, L. Tian, J. Wang, L. Jiang, K. Zhang, Water-CO2 wettability on sandstone surface with asphaltene adsorption: Molecular dynamics simulation, Fuel 360 (2024) 130558. https://doi.org/10.1016/j.fuel.2023.130558

[21] C.L. Brooks, D.A. Case, S. Plimpton, B. Roux, D. Van der Spoel, E. Tajkhorshid, Classical molecular dynamics, J. Chem. Phys. 154 (2021) 10. https://doi.org/10.1063/5.0045455

[22] D.C. Rapaport, The art of molecular dynamics simulation, Cambridge University Press, Cambridge, 2004.

[23] I. Omelyan, I. Mryglod, R. Folk, Optimized Verlet-like algorithms for molecular dynamics simulations, Phys. Rev. E 65 (2002) 056706. https://doi.org/10.1103/PhysRevE.65.056706

[24] E. Hairer, C. Lubich, G. Wanner, Geometric numerical integration illustrated by the Störmer–Verlet method, Acta Numer. 12 (2003) 399–450. https://doi.org/10.1017/S0962492902000144

[25] D.C. Rapaport, The art of molecular dynamics simulation, Cambridge University Press, Cambridge, 2004.

[26] P.G. Huray, Maxwell's equations, John Wiley & Sons, Hoboken, 2009.

[27] M.S. Daw, M.I. Baskes, Embedded-atom method: Derivation and application to impurities, surfaces, and other defects in metals, Phys. Rev. B 29 (1984) 6443. https://doi.org/10.1103/PhysRevB.29.6443

[28] J.E. Lennard-Jones, Cohesion, Proc. Phys. Soc. 43 (1931) 461. https://doi.org/10.1088/0959-5309/43/5/301

[29] M.H. Müser, S.V. Sukhomlinov, L. Pastewka, Interatomic potentials: Achievements and challenges, Adv. Phys. X 8 (2023) 2093129. https://doi.org/10.1080/23746149.2022.2093129

[30] J.E. Lennard-Jones, Cohesion, 43 (1931) 461. https://doi.org/10.1088/0959-5309/43/5/301

[31] LAMMPS Documentation, Compute group/group. https://docs.lammps.org/compute_group_group.html (accessed 1 December 2025).

[32] A.K. Rappé, C.J. Casewit, K. Colwell, W.A. Goddard

III, W.M. Skiff, UFF, a full periodic table force field for molecular mechanics and molecular dynamics simulations, J. Am. Chem. Soc. 114 (1992) 10024–10035. https://doi.org/10.1021/ja00051a040

[33] S.L. Mayo, B.D. Olafson, W.A. Goddard, DREIDING: A generic force field for molecular simulations, J. Phys. Chem. 94 (1990) 8897–8909. https://doi.org/10.1021/j100389a010

[34] S. Pal, K.V. Reddy, Molecular dynamics for materials modeling: A practical approach using LAMMPS platform, CRC Press, Boca Raton, 2024. https://doi.org/10.1201/9781003323495

[35] M. Sedghi, L. Goual, W. Welch, J. Kubelka, Effect of asphaltene structure on association and aggregation using molecular dynamics, J. Phys. Chem. B 117 (2013) 5765–5776. https://doi.org/10.1021/jp401584u

[36] B. Peng, et al., Molecular dynamics simulations of aggregation and viscosity properties of model asphaltene molecules containing a polycyclic hydrocarbon nucleus with toluene additive under shear interactions, RSC Adv. 14 (2024) 2577–2589. DOI: 10.1039/D3RA06483B

[37] S. Tazikeh, A. Shafiei, T. Yerkenov, A. Abenov, N. Seitmaganbetov, T.S. Atabaev, A systematic and critical review of asphaltene adsorption from macroscopic to microscopic scale: Theoretical, experimental, statistical, intelligent, and molecular dynamics simulation approaches, Fuel 329 (2022) 125379. https://doi.org/10.1016/j.fuel.2022.125379

[38] B. Zhu, Q. Hu, J. Zhang, The effect of water on asphaltene aggregation and viscosity of crude oil: A MD simulation study, in: Proc. 9th Int. Conf. Adv. Energy Resour. Environ. Eng. (ICAESEE 2023), Atlantis Press, 2024, pp. 407–413.

[39] R. Petuya, Á. Gómez, L. Martínez, C. Vega, Molecular dynamics simulations of asphaltene aggregation: Machine-learning identification of representative molecules, molecular polydispersity, and inhibitor performance, ACS Omega 8 (2023) 4862–4877. https://doi.org/10.1021/acsomega.2c07120

[40] S. Ahmadi, A. Khormali, Y. Kazemzadeh, A critical review of the phenomenon of inhibiting asphaltene precipitation in the petroleum industry, Processes 13 (2025) 126. DOI: 10.3390/pr13010212

[41] A. Ghamartale, Molecular-Scale Mechanistic Investigation of Asphaltene Precipitation and Deposition Control Using Chemical Inhibitors, Ph.D. Thesis, Memorial University of Newfoundland, St. John's, 2022.

[42] B. Liu, J. Li, C. Qi, X. Li, T. Mai, J. Zhang, Mechanism of asphaltene aggregation induced by supercritical CO_2: Insights from molecular dynamics simulation, RSC Adv. 7 (2017) 50786–50793. DOI: 10.1039/C7RA09736K

[43] S. Ansari, M. Rahimi, A. Beheshti, M. Rezaei, N. Mohamadian, A. Mohammadi, Experimental measurement and modeling of asphaltene adsorption onto iron oxide and lime nanoparticles in the presence and absence of water, Sci. Rep. 13 (2023) 122. https://doi.org/10.1038/s41598-022-27335-z

[44] N.N. Nassar, A. Hassan, P. Pereira-Almao, Metal oxide nanoparticles for asphaltene adsorption and oxidation, Energy Fuels 25 (2011) 1017–1023. https://doi.org/10.1021/ef101230g

[45] D. Chen, Y. Yang, Y. Li, X. Cui, J. Zhang, Influence of temperature on the adsorption and diffusion of heavy oil in quartz nanopore: A molecular dynamics study, Energies 15 (2022) 5870. https://doi.org/10.3390/en15165870

[46] X. Liu, Y. Gao, H. Sun, C. Liu, Y. Li, Effect of temperature on the aggregation kinetic and interaction mode of asphaltene in toluene–heptane system at molecular level using molecular dynamics (MD) simulation, J. Mol. Liq. 384 (2023) 122167. https://doi.org/10.1016/j.molliq.2023.122167

[47] M. Li, Y. Tian, C. Wang, C. Jiang, C. Yang, L. Zhang, Effect of temperature on asphaltene precipitation in crude oils from Xinjiang oilfield, ACS Omega 7 (2022) 36244–36253. https://doi.org/10.1021/acsomega.2c03630

[48] A. Bidram, M. Rahimi, M. Hekmatifar, The effect of temperature on asphaltene transformation and agglomeration in oil pressure tank systems under injection of carbon dioxide in a porous structure: A molecular dynamics study, J. Mol. Liq. 414 (2024) 126268. https://doi.org/10.1016/j.molliq.2024.126268